Journal of GeoEngineering, Vol. 17, No. 4, pp. 221-230, December 2022
http://dx.doi.org/10.6310/jog.202212_17(4).5

EFFECT OF NANOCLAY ON EROSION OF EMBANKMENT DAMS; AN INVESTIGATION THROUGH IMAGE PROCESSING

S. Mohamad A. Zomorodian [1], Mohamad J. A. Noghab [2], Masih Zolghadr [3], Mehrad Kamalzare [4*]

ABSTRACT

Overtopping erosion is one of the main causes of catastrophic failure of earth dam. One of the common preventive methods is to grout or add chemicals to the embankment soil. In this study, nanoclay which is devoid of any environmental detrimental effects was utilized. Erodibility of samples contained nanoclay with 0, 1, and 1.5 weight percent of dry soil and curing time of 0, 7, 14, 28 days were investigated using an image processing technique. To make a comparison between traditional and modern additives, a sample containing bentonite clay with 5 weight percent of dried soil was considered. The results showed positive effect of nanoclay on erodibility reduction of the soil. The sample with 1 percent nanoclay with 14 days curing time showed the highest improvement of the soil erodibility characteristic. Increasing the curing time to 14 days reduced the erodibility of all samples, thereafter it had no significant effect. Comparison of traditional and modern additives reveals that the erodibility of the sample containing 5 percent bentonite clay was about 10 times lower than that of the 1 percent nanoclay.

Key words: Erosion, Nanoclay, Image processing, Embankment dam, Bentonite.

1. INTRODUCTION

The integrity of the state and national system of embankment dams and levees is a crucial component in ensuring the safety of protected communities in any country. Levees are constructed along water courses to provide protection against floods while dams are constructed to form reservoirs to store water for urban, industrial or agricultural consumptions. The failure of such systems due to natural or man-made hazards can have monumental repercussions, sometimes with dramatic and unanticipated consequences on human life, property and the economy of the states and countries. These man-made structures generally serve as a barrier to prevent and reduce the risks of flooding parallel or perpendicular to flow direction. Depending on the purpose of the construction, it is made in un-compacted, semi-compacted, compacted, and hydraulic fill conditions with different percentages of water content. Therefore, identifying the potential engineering threats and design challenges is crucial for the stability and integrity of the structure as well as for providing appropriate preventative solutions.

Both overtopping and internal erosion or piping have always posed problems in several different embankment dams around the world. Internal erosion has been identified as the second leading cause of earth dam failures in the world. About 30% of earth dam failures have occurred due to internal erosion (Guy and Shawki 1992). Hydraulic erosion is a complicated phenomenon and depends on many different parameters. Although much work has been done to simulate erosion in the field of computer graphics, there has been limited validation. This is mostly because of limitations of current laboratory measurement methods, especially in regard to the surface erosion, which is can be caused by overtopping. Kamalzare *et al.* (2016) using geotechnical centrifuge testing, developed tools and introduced a new visualization methodology that would improve the understanding of the process of embankment failure because of erosion and reduce the risk of failure.

Since fine-grained soils play a dominant role in earth structures, researchers have investigated the effects of conventional additives such as, bentonite, lime, calcium compounds etc. on the geotechnical properties of these type of soils (Ahn and Jo 2009; Lajurkar *et al.* 2016; Zhang *et al.* 2017; Spangoli 2018). In the recent years, nanomaterials, which have unique characteristics and have undergone fundamental changes in a variety of engineering sciences, have drawn the attention of researchers as a method to improve soil properties. Many agencies have invested large amounts of budget on nanotechnology research. Of particular importance is this new technology in the present age, approximately $5.5 billion are spent on investment in nanotechnology research annually. In the recent years, large number of studies have been conducted on the application of nanocomposites, especially nanoclay, to improve different geotechnical properties of soils. Padidar *et al.* (2017) investigated the effect of nanoclay on the stabilization of sandy soil under wind erosion. They conducted experiments with baseline (water) and nanoclay solutions, which showed the significant effect of nanoclay on increasing soil resistance to wind erosion. Taghavi *et al.* (2018) examined the impact of nanoclay on the seepage through earth dams. They used two nanoclay contents (0.5%, 1%) and three thicknesses (10, 5, and 3 cm) to create an impermeable layer (blanket) on the upstream side slope. Using GeoStudio model (SEEP/W), they examined the seepage rate in each test. The results indicated the significant effect of nanoclay on seepage reduction.

Manuscript received July 12, 2022; revised September 11, 2022; accepted November 1, 2022.
[1] Associate Professor, Department of Water Engineering, College of Agriculture, Shiraz University, Shiraz, Iran.
[2] M.Sc. Hydraulic Structures, Department of Water Engineering, College of Agriculture, Shiraz University, Shiraz, Iran.
[3] Assistant Professor, Department of Water Sciences Engineering, College of Agriculture, Jahrom University, Jahrom, Iran.
[4*] Associate Professor (corresponding author), Civil Engineering Department, California State Polytechnic University, Pomona, California, USA (e-mail: mkamalzare@cpp.edu).

Abbasi *et al.* (2018) investigated the effect of nanoclay on the stabilization of dispersive clay soils with low and high plasticity properties. Using Pin-hole test, they studied samples containing 2, 1, 0.5, 0.25, 0 percent by weight of dry soil with three curing times (1, 3, 7 days). The results showed that the addition of nanoclay significantly reduced the swelling potential. It was reduced, however, to a higher extent in clay soils with higher plasticity. Zomorodian and Momen (2018) investigated the effect of nanosilica particles on the erosion of dispersive soils. The results showed the significant effect of nanosilica particles on reducing erodibility as well as the direct effect of curing time on nanosilica performance. Asakereh and Avazeh (2016) examined the effect of nanoclay on dispersive soil behavior. They found that adding a small percentage of nanoclay to the soil can partially improve soil dispersivity but adding too much increases the dispersivity potential.

Baziar *et al.* (2018) investigated the effect of nanoclay on hydraulic conductivity in the core of an earth dam made of dense sandy clay. They made two samples using Kaolinite clay and Firuzkooh sand with a ratio of 1 to 9 and 1 to 4, respectively. Then, they examined the effect of adding nanoclay contents of one to four percent. Results showed that adding nanoclay up to 3% (as the optimum percentage) can significantly reduce the hydraulic conductivity to reach an acceptable value for the earth dam cores. Badv and Hoseinzade (2018) investigated the effect of adding nanoclay on improving clay properties of Nazlou, Orumieh and Firoozkooh sand. The results showed that the nanoclay raised the plasticity index (PI) and optimum water content (w_{opt}) and reduced the maximum dry weight ($\gamma_{d\text{-max}}$) of Nazlou clay. In addition, it reduced the coefficient of hydraulic conductivity of both soils to the standard level required for clay blanket construction but, in sand, this value did not reach the standard level. Zomorodian *et al.* (2017) studied the effect of nanoclay and nanosilica additives on soil resistance improvement in petroleum contaminated and clean soils. Adding 1% nanoclay and 1.5% of nanosilica to clean soil showed a significant effect on soil erosion recovery. They reported that generally nanoclay has a better weight percent for both contaminated and clean soils compared with the weight percent of nanosilica. Tabarsa *et al.* (2018) examined the effect of nanoclay on improving the properties of loess. For this purpose, they added different percentages of nanoclay (0.2% to 3% by weight) to the loess soil. Results showed enhancement of loess properties such as plasticity, strength, and stiffness of the soil in all samples. The best results, however, were obtained for the sample with 2% nanoclay content.

Several methods have been developed to investigate the trends and factors affecting erosion. Including Flume Test (Shaikh *et al.* 1988), Channel Testing (Arulanandan 1983), Rotary Cylinder Test (Chapuis and Gatien 1986), Hole Erosion Test (HET) (Maranha das Neves 1989), Jet Erosion Test (JET) (Hanson 1991), and Solt Test (Wan and Fell 2004).

Wahl (2010) compared HET and JET tests and argued that the JET offers the most capability for investigating the properties of a wide range of soils, while the HET is particularly desirable for erosion conditions. Therefore, he emphasized the choice of testing, appropriate to the mechanism of erosion for more accurate results and efficiency. Elkhoy *et al.* (2015) investigated erosion in embankments with different percentages of sand, silt and clay under a new experimental method. They found that a slight change in clay content affected the erosion rate significantly.

Due to the complexity of the surface phenomenon of overtopping erosion and its significant role in embankment breach and failure, as well as the limitations of mathematical solution to reasonably quantify or predict the erosion surface, there is an essential demand for a new approach to indirectly, using image processing, and artificial neural network (ANN), to quantify and analyze the surface erosion phenomenon. This is mainly a complex matter, due to the fact that the geo-metry and shape of the eroded surface are functions of time, as well as several other factors such as flow rate, the exact shape and size of the soil particles on the surface in contact with the water flow. The soil structure and the exact pattern of how each individual particle is in contact with other particles within the upper few centimeters of soil at each moment of time can all affect the geometry and the amount of surface erosion. This study was conducted to gain a proper understanding of the erosion process and to provide effective solutions to control and reduce the damages caused by overtopping erosion. The effects of nanoclay additive on embankment erosion was studied through image processing technique as a novel approach in this field of study. Bentonite, as a traditional additive is also considered to make a comparison with modern nanoclay materials.

2. MATERIALS AND METHODS

2.1 Nanoclay

In this study, Montmorillonite nanoclay was used. This nanoclay is a product of Sigma-Aldrich Co., and its physical properties are listed in Table 1. The results of the chemical analysis on the soil is presented in Table 2.

Table 1 Physical characteristics of Montmorillonite nanoclay

Parameter	Value/Description
Specific Weight (kg/m^3)	300 ~ 370
Particle size (nm)	1 ~ 2
Color	Light yellow
Water content (%)	1 ~ 2
Electrical conductivity (MV)	25
Ion exchange coefficient (me/100gr)	48

Table 2 Chemical analysis of Montmorillonite nanoclay

Chemical component	Percentage (%)
Na_2O	0.98
MgO	3.29
Al_2O_3	19.60
SiO_2	50.95
K_2O	0.86
CaO	1.97
TiO_2	0.62
Fe_2O_3	5.62
Loss of ignition (LOI)	15.45

2.2 Soil

The soil studied in this study was a mixture of sand with uniform grain size distribution and a soil passing through No. 4 sieve (4.75 mm) from Bajajah in the Central District of Shiraz County, Fars Province in southern Iran (with a mixing ratio of 4 to 1) to produce an erodible mixture. The soil was classified as silty sand

(SM) in accordance with the Unified Soil Classification System.

The grading experiments (D6913), standard Proctor compaction (D698), Atterberg limits (D4318) and specific gravity of solids (G_s) tests (D854) were all performed according to ASTM standard. Figure 1 shows the grain size distribution curve (including the results of hydrometer test for the fine-grained portion), while Fig. 2 shows the compaction curve results. Table 3 shows the physical properties of the soil.

The soil mass required for each experiment was calculated according to the final embankment height and the maximum dry density (from the standard Proctor test). To prepare the laboratory physical soil samples, water content = $w_{opt} \pm 3\%$ was added to the soil. The samples were then placed in a sealed container for 24 hours to achieve a uniform moisture content.

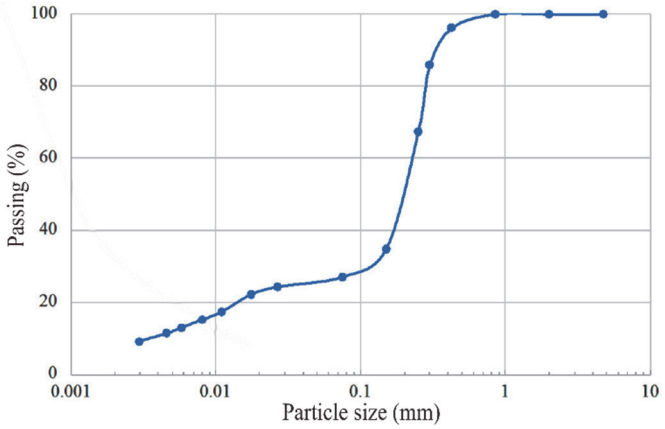

Fig. 1 Particle-size distribution curve for SM soil material investigated

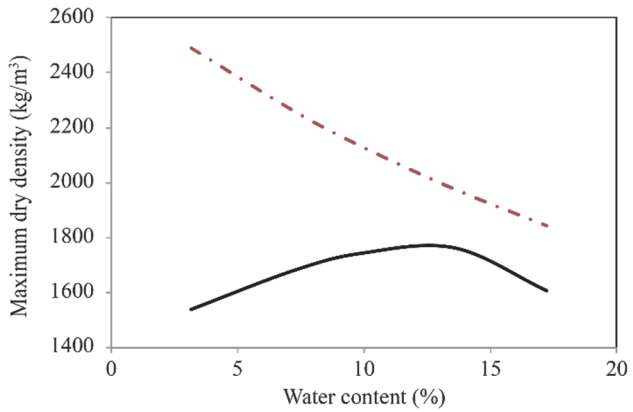

Fig. 2 Soil compaction curve (solid line) and the zero-air-void curve (dashed line)

Table 3 Physical Properties of the Soil

Parameter	Value
G_s	2.70
$\rho_{d\text{-max}}$	1770 kg/m^3
w_{opt}	12.8%
D_{50}	0.19 mm
LL	Nonplasticity
PL	Nonplasticity

As it was mentioned the effect of curing time of the nanoclay was also investigated in this research. Therefore, after adding the above-mentioned water content to the samples containing nanoclay, they were kept in containers for one, two, and four weeks. Table 4 shows the values of the maximum dry density, and the optimum water content for each sample.

Table 4 Maximum dry density and optimum water contents

$\rho_{d\text{-max}}$ (kg/m^3)	w_{opt} (%)	Sample
1770	12.8	Control
1847	13	1% Nanoclay
1862	12.3	1.5% Nanoclay
1910	13	5% Bentonite
1895	13.6	10% Bentonite
1873	14	15% Bentonite

3. EXPERIMENT SETUP

The experiments were carried out in a concrete flume, with 0.5 m wide, 0.5 m deep and 16.5 m long. Figure 3 shows a schematic view of the flume.

As it is shown in Fig. 3, a portion of the flume was replaced by glass to observe and record the erosion process. The embankment model was constructed behind the glass section of the flume with dimensions of 55 × 15 × 15 cm and with 1:1 and 2:1 upstream and downstream side slopes respectively. To reduce the amount of required soil mass for the construction of each embankment, the width of the flume was decreased by installing a solid steel embankment in the flume, with dimensions of 55 × 35 × 15 cm and same upstream and downstream side slopes to the ones for embankment. Since erosion is inherently a time-consuming phenomenon, to simulate and accelerate the occurrence of the piping, a 1.2 cm diameter steel rod was placed at the bottom of the flume and adjacent to the glass prior to placement and compacting the first lift of the embankment. Placement and compaction of the second and third layers were similarly performed (Fig. 4).

After construction of the embankment, water inundated the flume and began to rise. To keep a constant reservoir head, a 30 cm wide side spillway was installed at the upstream of the embankment (Fig. 5). The side spillway was a rectangular sharp crested with a height of 13.5 cm from the bottom of flume. A control valve was used to regulate the desired discharge to the flume. The flow rate used for all tests was constant at 1.5 liters per second. Once the water surface reached the elevation of 14 cm, the steel

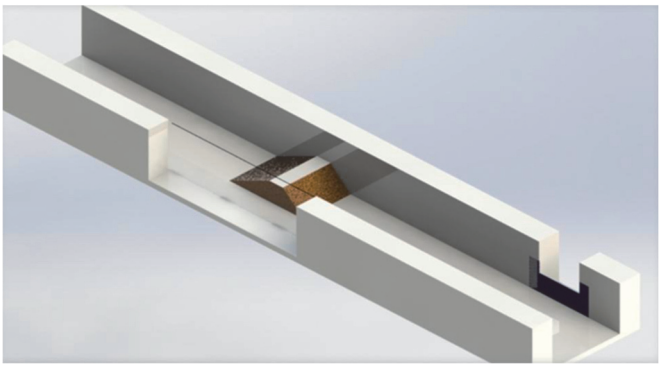

Fig. 3 Schematic overview of the concrete flume

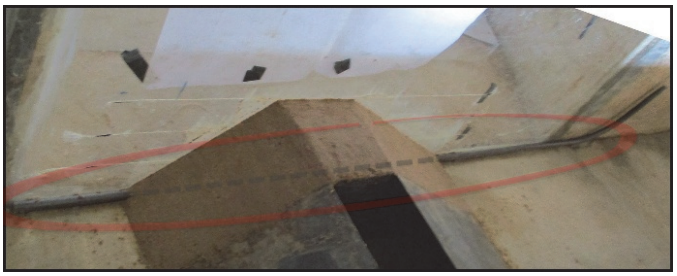

Fig. 4 Steel rod installation

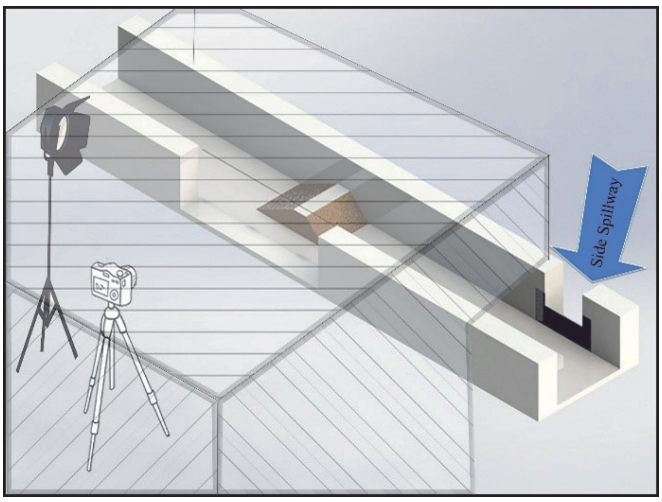

Fig. 5 Camera and recording equipment setup (the gray area is covered by curtains to eliminate unwanted light reflection)

rod was pulled out and the camera, in front of the glass face of the flume (as shown in Fig. 5), began to record images. The experiments were stopped when the surface of the water was separated from the embankment surface due to erosion.

4. IMAGE PROCESSING

An HD camcorder with a frame rate of 30 frames per second was used to record images. To create a more uniform illumination and reduction of unwanted noise (unwanted light reflection), the recording area was covered by a curtain and a 30-watt spotlight was used as the light source under the curtain. Potassium permanganate solution was also used as a dye to differentiate between eroded and intact soils. Image processing was performed using the Canny algorithm. Many algorithms have been proposed for detecting edges in image processing. The basis of many of these algorithms is to differentiate the image intensity function. Canny algorithm was introduced in 1983 (Canny 1983) and received a great deal of popularity, where is now widely used in industry as a detector.

In this study images were recorded at intervals of 5 seconds in full RGB color and then went under different steps of image processing. Figure 6 provides a brief overview of the image processing operations performed in this study as an example. Figure 6(a) shows a frame of the video recorded from the experiment. The RGB color model consists of three colors: Red, Green, and Blue. This RGB model was then converted to 8-bit gray level (Fig. 6(b)). The 8-bit gray area of each pixel of the image can have an optical intensity of between 0 and 255, with 0 representing black and 255 representing white. In the next step the thresholding operation is performed to differentiate the borders and facilitate segmentation and editing (Fig. 6(c)). By specifying a value of brightness as the threshold, "Threshold Function" turned the brightness value of all pixels less than that, to zero. It turns the higher values into one, where 0 represents black and 1 represents white. This changes the images to a binary one (black and white) via a thresholder. The image is then processed by the canny edge detection algorithm, where the edges of all objects in the image are shown in white, of which only the eroded lines are considered, and the rest being changed to white as noise lines (Fig. 6(d)) and were removed in the final step by applying a few filters. The resulting image is the output of the image processing operation used to convert the image to a diagram (Fig. 6(e)).

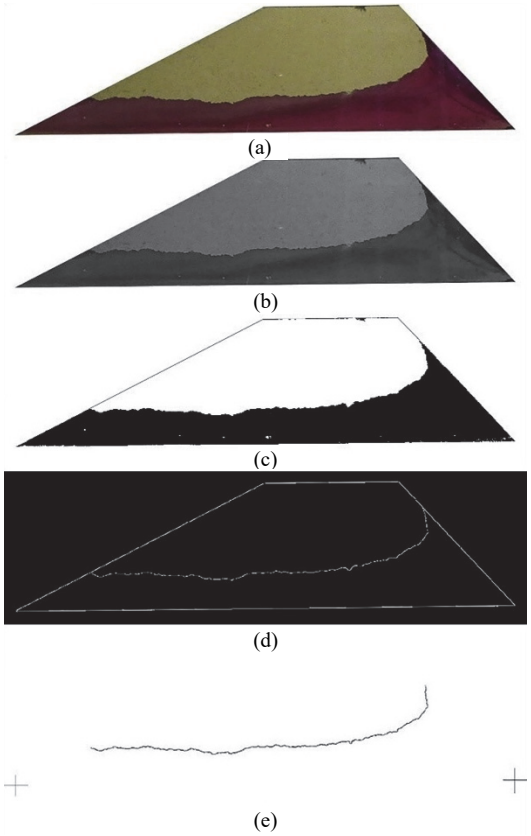

Fig. 6 Image processing steps: (a) recorded RGB image; (b) gray scale; (c) thresholding; (d) edge detection; (e) noise removal and erosion line separation

5. MATHEMATICAL RELATIONS

To investigate the relationship between parameters such as density and time elapsed since the beginning of the experiment, images of erosion lines obtained by image processing were analyzed with Artificial Neural Network (ANN) and Response Surface Methodology (RSM).

5.1 Artificial Neural Network (ANN)

To predict the bathymetry of the erosion line, digitized outputs of the image processing technique were used to train the ANN.

To find the best mapping between input and output values, a grid was designed by 2 hidden layers, each made with 10 neurons and 3 sigmoid tangent transfer functions, sigmoid logarithm and softmax functions were used. To select the best network, the mean squared error values of the networks were compared and the least error network was selected as the optimal network.

5.2 Response Surface Methodology (RSM)

The RSM which was used for data analysis, is a set of mathematical methods that determine the relationship between one or more response variables with several independent variables. The purpose of the RSM is to optimize the response (output variable) that is affected by several independent variables (input variables). This method is preferable to the ANN as it makes it possible to estimate the relationship between input variables and response as a mean to determine the sensitivity of the response to each of the factors (input variables).

6. RESULTS AND DISCUSSION

6.1 Image processing time intervals and curing time

Given the results of the compaction test, optimum water content was added to the control sample, while preparation and experimentation were being performed as described above. Figure 7 depicts the erosion lines obtained from image processing with no curing time at 5, 10, and 20 sec intervals. Since the effects of the nanoclay samples curing-time was of interest of this study, its effect on the control sample was also investigated. Figure 8 shows the erosion lines of the control sample produced by image processing with one-week curing time. Table 5 shows the duration and properties of the control tests (baseline soil sample).

It can be seen from Table 5 that the curing time raised the duration of the experiments, however, it did not lead to any significant difference compared to samples with more than one week curing time.

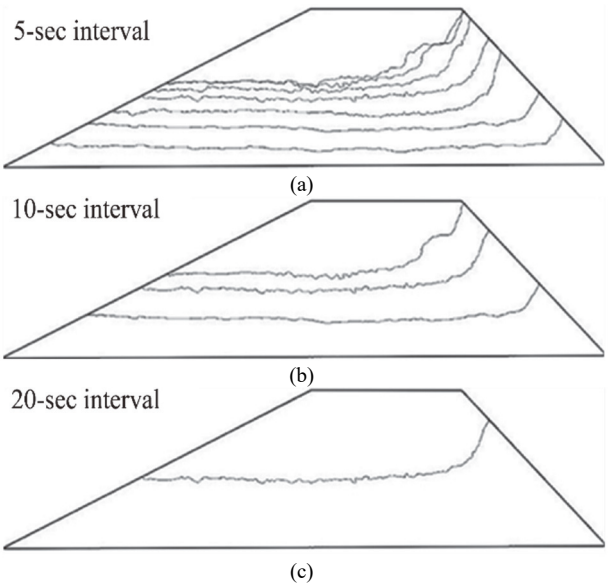

Fig. 7 Erosion lines obtained from image processing of untreated control test with different intervals

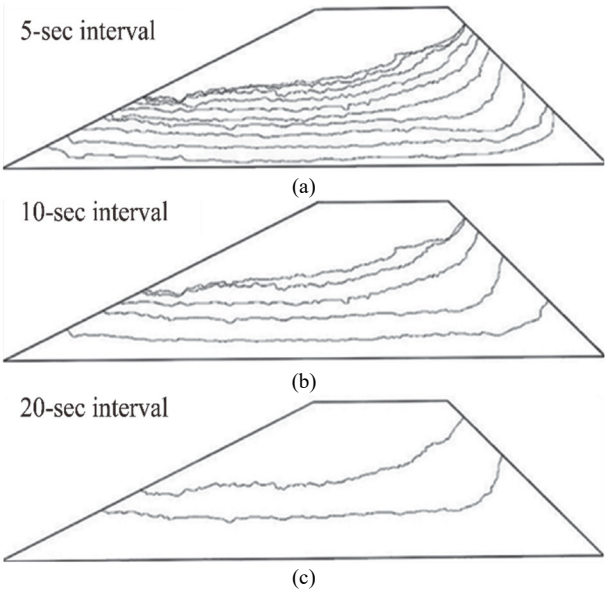

Fig. 8 Erosion lines bathymetry obtained from image processing of control experiment with seven days curing time and different intervals

Table 5 Control tests on the baseline soil sample

Water content (%)	Curing time (day)	Experiment duration (sec)
12.8	0	35
12.8	7	50
12.8	14	45
12.8	28	49

6.2 Comparison of image processing produced erosion lines with diagrams of digitization

To compare the bathymetry of erosion lines at different time intervals with one another, images were digitized. Figure 9 shows the image and diagram plotted using digitized data for the baseline test without curing time. According to Fig. 9, the graph plotted by the data obtained from the digitization of the image is highly consistent and therefore, these data can be used to analyze and compare erosion in different samples.

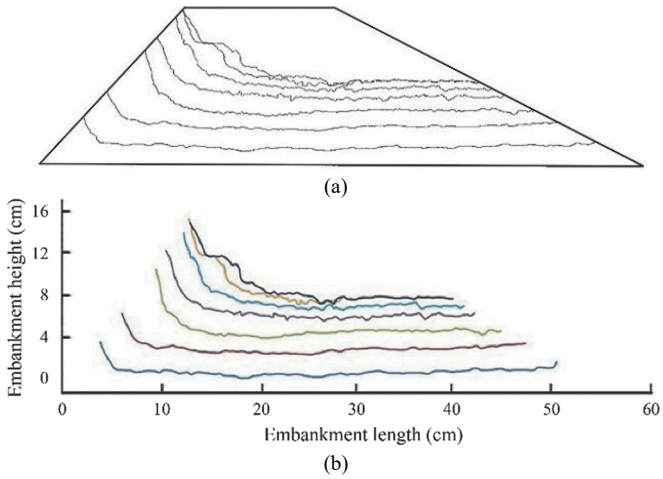

Fig. 9 (a) Image of erosion lines bathymetry with a time interval of 5 seconds; (b) diagram plotted by data obtained from digitization of erosion lines image

6.3 Effects of amounts of nanoclay content on the erosion

Samples containing nanoclay were tested with two different percentages of 1% and 1.5% by weight and with curing time of 0, 7, 14, and 28 days. The percentages of nanoclay content and optimum values in this study were chosen based on the results of previous studies (Arabani *et al.* 2012, Neethu and Remya 2013, Zomorodian *et al.* 2017). The optimum water content of each soil mixture was used to prepare each associated model. Table 6 shows a summary of the tests performed for this phase of the study.

Figure 10 shows an overview of the erosion line bathymetry for samples with one percent nanoclay, and different curing time, which Fig. 11 present similar graphs for the results of the tests on the specimens with 1.5% nanoclay. For the specimens with 1.5% nanoclay no test was performed with zero curing time. The results in both figures are shown only for the 10 second time intervals as an example.

Table 6 Experiment's Duration of nanoclay containing samples

Nanoclay content (%)	Water content (%)	Curing time (day)	Experiment duration (sec)
1	13	0	145
1	13	7	185
1	13	14	315
1	13	28	250
1.5	12.3	7	200
1.5	12.3	14	240
1.5	12.3	28	195

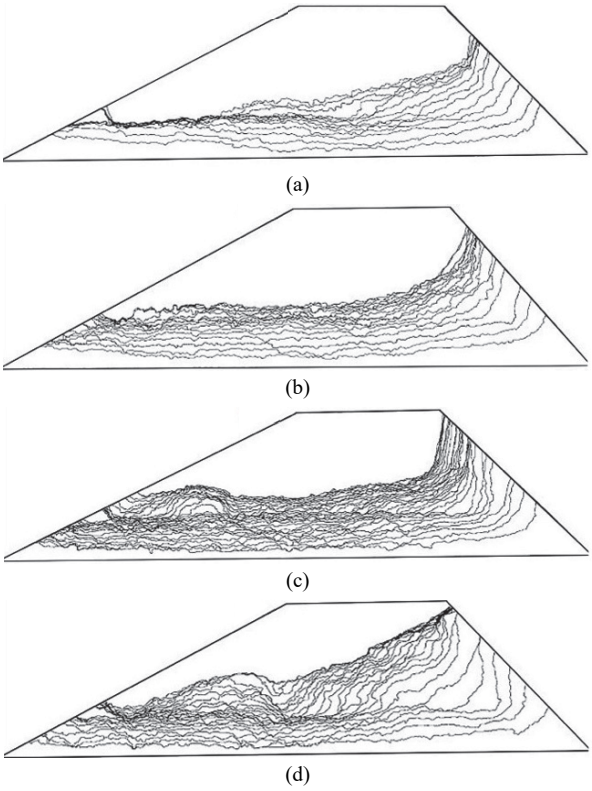

Fig. 10 Bathymetry of erosion lines of 10 sec time interval for 1% nanoclay content with a curing time of (a) 0 days, (b) 7 days, (c) 14 days, and (d) 28 days

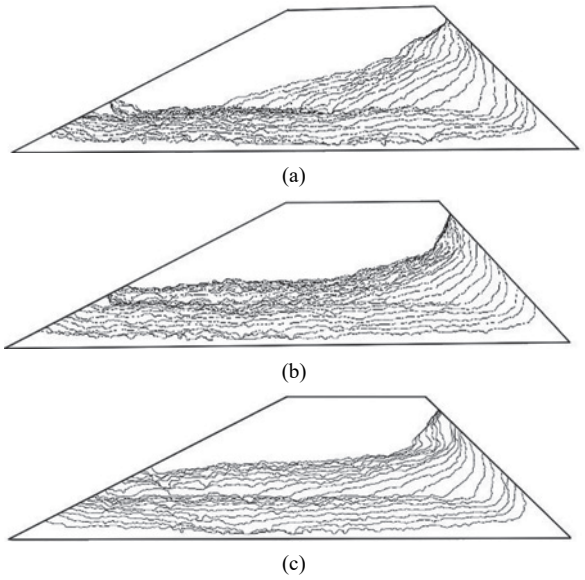

Fig. 11 Bathymetry of erosion lines of 10 sec time interval for 1.5% nanoclay content with a curing time of (a) 7 days, (b) 14 days, and (c) 28 days

6.4 Effect of Different Bentonite Clay Contents on Control Samples

Models built from samples containing 5%, 10%, and 15% bentonite clay were also examined to compare the effect of traditional (bentonite) and modern (nanoclay) additives. Bentonite samples were kept for several days in isolated containers to gain a uniform moisture. No curing time was then considered for these samples. The bathymetry of the erosion lines obtained from image processing for each experiment are shown in Fig. 12 while the duration of the experiments is presented in Table 7.

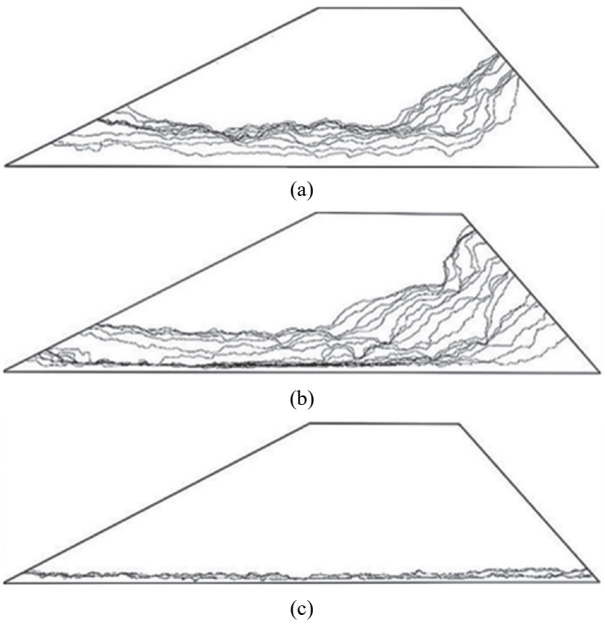

Fig. 12 Bathymetry of erosion lines of samples containing various percentage of bentonite (5-min interval image processing): (a) 5% bentonite; (b) 10% bentonite; (c) 15% bentonite

Table 7 Recording duration for samples containing bentonite

Bentonite content (%)	Water content (%)	Experiment duration (min)
5	13.0	60
10	13.6	100
15	14.0	240

As it can be seen from the erosion line images shown in the above figure, and experiment duration presented in Table 7, there is a direct relationship between bentonite content growth and erodibility reduction or cohesion rise, and the soil erosion resistance. In the two samples containing 5% and 10% bentonite, the stopping condition occurred (the separation of water surface from the soil surface). However, in the sample containing 15% bentonite, due to minor erosion after 4 hours, recording was cut without having interruption condition satisfied. The bentonite effect can be attributed to the increased cohesion of the soil particles. As it can be seen in Fig. 12(a), there is clearly a higher amount of uneven surface in the erosion lines than in the control sample, indicating a lump erosion of the particles due to enhanced cohesion. In the samples containing 10% (b) and 15% (c) bentonite, these distortions have become fewer due to inter-particle cohesion multiplication, so that in the sample containing 15% bentonite, the hydraulic gradient is not capable of causing erosion and disintegrating the embankment.

6.5 Comparison of Bentonite and Nanoclay Clays Effect on Erosion of Baseline Sample

The sample containing 1% nanoclay cured for 14 days, had the best performance (Figs. 10 and 11), which were compared with the sample containing 5% bentonite. As it can been from Tables 6 and 7, however, the duration of these two experiments were quite different; indicating that bentonite clay has a greater effect on the cohesion of the samples and consequently improving the erodibility of soil. However, the difference in the percentages of these two additives, as well as the curing time should also be taken in to account. Therefore, the difference in the duration of the experiment cannot be solely attributed to the influence of the type of additive.

7. PRESENTED MODELS AND ANN RESULTS

Data obtained from digitizing images of the erosion lines of the samples containing nanoclay with 7, 14, and 28 days curing time were analyzed via RSM and ANN. Four equations and one corresponding network were developed. Tables 8 shows the estimated coefficient of determination for proposed models, while ANN and the equations accuracy in terms of RMSE are presented in Table 9.

Table 8 Coefficients of determination for estimated equations

Source	Predicted R^2	Adjusted R^2	Sequential p-value
Two fractional interaction	0.7531	0.7530	< 0.0001
Quadratic	0.8485	0.8484	< 0.0001
Cubic	0.9182	0.9181	< 0.0001
Cubic (square root)	0.9427	0.9426	< 0.0001

Table 9 Evaluation of equations and ANN

Equations and ANN	RMSE
Two fractional interactions (2FI)	0.0883
2nd order equation	0.0691
3rd order equation	0.0508
3rd order equation (2nd root)	0.0718
ANN	0.0205

As it can be seen from Table 8, the 3rd degree equations (3rd degree and 3rd degree with 2nd root conversion) have the highest consistency with observed data. For further investigation and checking the compatibility of the equations and the network with observed data, different erosion line bathymetries of each equation were plotted at different time intervals. Figure 13 shows examples of these diagrams. Vertical and horizontal axes are the dimensionless height and length of the embankment on these figures. To obtain dimensionless values, any desired height (y) and length (x) were normalized by the initial corresponding values of the embankment respectively (15 cm as y' and 55 cm as x').

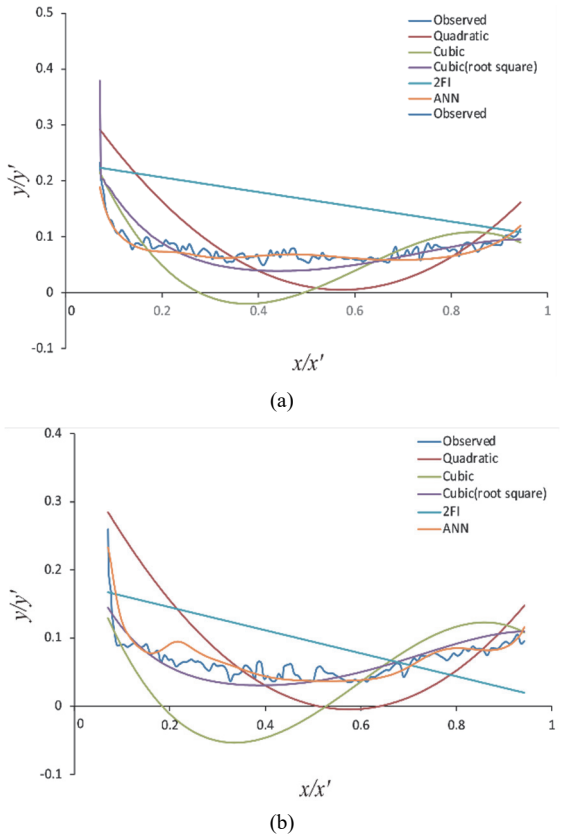

Fig. 13 Estimated erosion lines for the sample; (a) containing 1% nanoclay with a 14 day curing time; (b) containing 1.5% nanoclay with 28 days curing

8. SCANNING ELECTRON MICROSCOPE (SEM) PHOTO RESULTS

To further understand the performance of nanoclay, photography of three control samples, as well as samples containing one and six percent nanoclay were performed using a scanning electron microscope. Figure 14 shows images of the control soil and the 1% nanoclay containing samples.

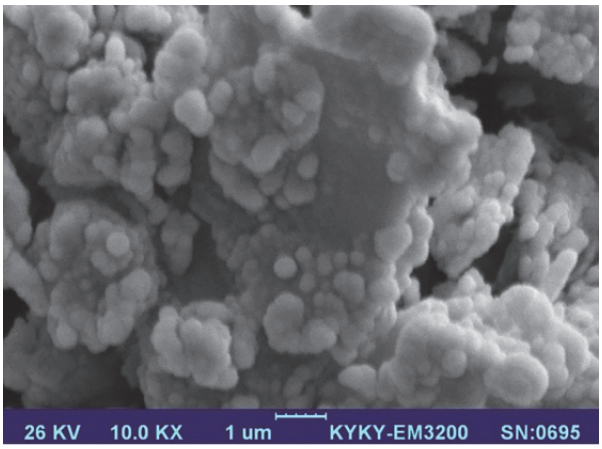

(a)

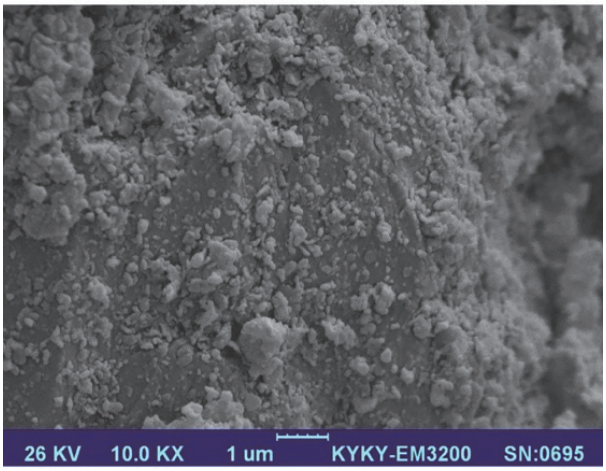

(b)

Fig. 14 SEM images at a magnification of 10,000 times: (a) control sample; (b) sample containing 1% nanoclay

It can be seen in Fig. 14 that the soil particles surface in the baseline sample have large voids, while the sample with 1% nanoclay content, is much more uniform with very smaller voids, indicating the influence of nanoclay on decreasing soil void ratio.

Figure 15 shows the nanoparticles in the sample containing 6% nanoclay with a magnification of 40,000 times. The size of the smallest particle (nanoclay) specified in the image is 37 ~ 79 nm, while the manufacturer claims their dimensions to be 1 ~ 2 nm. This can be due to the fact that nanoclay particles are highly susceptible to flocculation due to their high surface charge and specific surface, which can lead them to form edge-to-edge and edge-to-face bonds.

Therefore, there should be an optimum percentage for nanoclay content that would create a chain, surround the soil particles and result in the over increase of soil cohesion, and consequently reduction of soil erodibility. This chain can fill the voids efficiently in the optimum content case. However, if the nanoclay content exceeds the optimum value not only no or minimal enhancement would be expected in nanoclay performance, but also it can be declined in some cases. This result from the tendency of nanoclay particles to bond together (flocculation) and reducing or even stopping their participation in soil cohesion enhancement resulting in void ratio escalation. Figure 16 illustrates how the nanoclay performs as described.

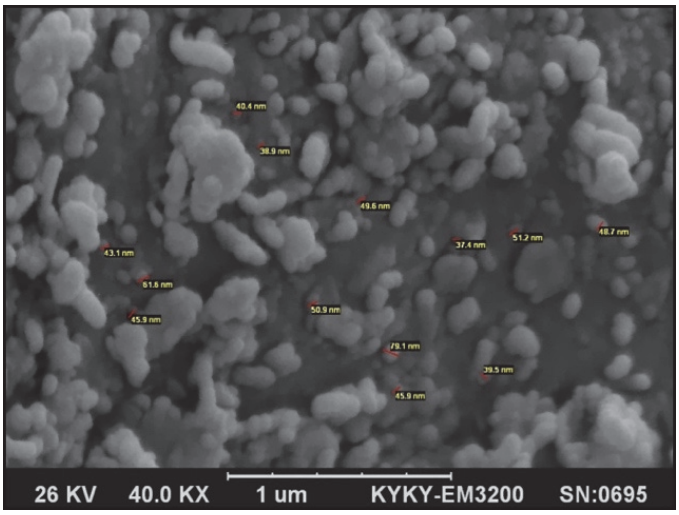

Fig. 15 Sample containing 6% nanoclay at 40,000 times magnification (sizes of nanoclay particles rages between 40 to 80 nm)

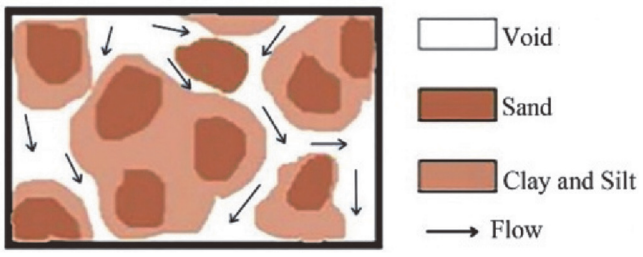

(a)

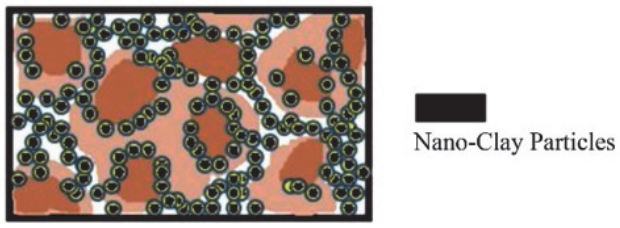

(b)

Fig. 16 Schematic of nanoclay particles performance: (a) soil with no additives; (b) soil containing nanoclay

In a number of studies regarding the effects of nanoclay and some other nano-materials additives on the geotechnical properties of different soils, similar results about the optimum percentage of additives were concluded, showing how the nanoclay/nanomaterials work in the micro and macro scales (Arabani *et al.* 2012; Majeed and Taha 2012; Mohammadi and Niazian 2013; Neethu and Reyma 2013; Bedv and Hoseinzade 2014; Tabarsa *et al.* 2017; Baziar *et al.* 2018).

9. CONCLUSION

The influence of nanoclay additives on surface erosion of embankment was investigated by employing the novel technique of image processing. A comparison with bentonite as a traditional additive was also conducted. The below specific conclusions can be drawn from this study:

1. Adding nanoclay to the soil enhances its resistance to erosion. In comparison with the sample with no additive, this improvement was found to be 4, 7, and 5 times for the samples containing 1% nanoclay, with 7, 14, and 28 days curing time respectively.
2. The impact of nanoclay on reducing erodibility rose slightly by increasing the curing time only up to a certain limit and with minimal effect after that.
3. At one week curing time, the sample containing 1% nanoclay showed a greater resistance against erosion in comparison to sample containing 1.5% nanoclay.
4. When the performance of nanoclay was compared to that of bentonite clay as a traditional additive, the sample containing 5% bentonite clay showed higher resistance to erosion, compared to samples that contained 1 or 1.5 percent nanoclay.
5. According to the SEM images, the flocculated nanoclay particles allows a better filling of the voids, as well as better uniformity and densification of the soil surface. This enhances resistance to soil to erosion.
6. The added nanoclay shows the best performance at an optimum percentage and its effects descends for lower or higher contents.

FUNDING

The authors received no funding for this work.

DATA AVAILABILITY

The data and/or computer codes used/generated in this study are available from the corresponding author on reasonable request.

CONFLICT OF INTEREST STATEMENT

The authors declare that there is no conflict of interest.

REFERENCES

Abbasi, N., Farjad, A., and Sepehri, S. (2018). "The use of nanoclay particles for stabilization of dispersive clayey soils." *Geotechnical and Geological Engineering*, **36**(1), 327-335. https://doi.org/10.1007/s10706-017-0330-9

Ahn, H.S. and Jo, H.Y. (2009). "Influence of exchangeable cations on hydraulic conductivity of compacted bentonite." *Applied Clay Science*, **44**(1-2), 144-150. https://doi.org/10.1016/j.clay.2008. 12.018

Arabani, M., Haghi, A.K., Mohammadzade Sani, A., and Kamboozia, N. (2012). "Use of nanoclay for improvement the microstructure and mechanical properties of soil stabilized by cement." *In Proceedings of the 4th International Conference on Nanostructures*.

Arulanandan, K. and Perry, E.B. (1983). "Perry Erosion in relation to filter design criteria in earth dams." *Journal of Geotechnical Engineering*, ASCE, **109**(5), 682-698. https://doi.org/10.1061/(ASCE)0733-9410(1983)109:5(682)

Asakereh, A. and Avazeh, A. (2017). "The effects of nano clay on dispersive soils behavior (Case Study of Minab City)." *Amirkabir Journal of Civil Engineering*, **49**(3), 153-156. https://doi.org/10.2206 0/ceej.2016.868

ASTM D698-12 (2021), Standard Test Methods for Laboratory Compaction Characteristics of Soil Using Standard Effort. https://doi.org/10.1520/D0698-12R21

ASTM D4318-17 (2018), Standard Test Methods for Liquid Limit, Plastic Limit, and Plasticity Index of Soils. https://doi.org/10.1520/D4318-17E01

ASTM D6913-04 (2017), Standard Test Methods for Particle-Size Distribution (Gradation) of Soils Using Sieve Analysis. https://doi.org/10.1520/D6913-04R09E01

ASTM D854-14 (2016), Standard Test Methods for Specific Gravity of Soil Solids by Water Pycnometer. https://doi.org/10.1520/D0854-14

Badv, K. and Hoseinzade, S. (2018). "The effect of admixing of nano-clay to nazloo clay and firoozkouh sand for clayey liner applications." *Sharif Journal of Civil Engineering*, **33.2**(4.1), 125-133. https://doi.org/10.24200/J30.2018.1257

Badv, K. and Hoseinzade, S. (2014). "Investigating the effect of nanoclay on the geotechnical behavior of the Uremia Nazluy clay and the Firuzkouh sand." *Eighth National Civil Engineering Congress*, Noushirvani Industrial University of Babol, Iran.

Baziar, M.H., Saeidaskari, J., and Alibolandi, M. (2018). "Effects of nanoclay on the treatment of core material in earth dams." *Journal of Materials in Civil Engineering*, ASCE, **30**(10), 04018250. https://doi.org/10.1061/(ASCE)MT.1943-5533.0002415

Canny, J. (1983). "Finding edges and lines in images." *Report AI-TR-720*, MIT Artificial Intelligence Laboratory, Cambridge, MA. https://dspace.mit.edu/handle/1721.1/6939

Chapuis, R.P. and Gatien, T. (1986). "An improved rotating cylinder technique for quantitative measurements of the scour resistance of clays." *Canadian Geotechnical Journal*, **23**(1), 83-87.

Elkholy, M., Sharif, Y.A., Chaudhry, M.H., and Imran, J. (2015). "Effect of soil composition on piping erosion of earth levees." *Journal of Hydraulic Research*, **53**(4), 478-487. https://doi.org/10.108 0/00221686.2015.1026951

Gutierrez, M.S. (2005), "Potential applications of nano-mechanics in geotechnical engineering." *Proceeding of the International Workshop on Micro-Geomechanics across Multiple Strain Scales*, Cambridge, UK, 29.

Guy, L.H. and Shawki, S. (1992). "Water dams and civilization." *World Bank Technical Paper*, **115**, 5-13.

Hanson, G.J., (1991). "Development of a jet index to characterize erosion resistance of soils in earth spillways." *Transactions of the American Society of Agricultural Engineers*, **34**(5), 2015-2020. https://doi.org/10.13031/2013.31831

Kamalzare, M., Zimmie, T.F., Cutler, B., and Franklin, W.R. (2016). "New visualization method to evaluate erosion quantity and pattern." *Geotechnical Testing Journal*, **39**(3), 1-16. https://doi.org/10.1520/GTJ20140226. ISSN 0149-6115

Lajurkar, S., Golait, Y.S., and Khandeshwar, S.R. (2016). "Effect of calcium chloride on engineering properties of black cotton soil." *International Journal of Innovative Research in Science, Engineering and Technology*, **2**(5), 1766-1771.

Majeed, Z.H. and Taha, M.R. (2012). "Effect of nanomaterial treatment on geotechnical properties of a penang soft soil." *Journal of Asian Scientific Research*, **2**(11), 587-592. https://archive.aessweb.com/index.php/5003/article/view/3399

Maranha das Neves, E. (1989). "Analysis of crack erosion in dam cores the crack erosion test." *de Mello Volume, Sao Paulo,*

Brazil, 284-298.

Mohammadi, M. and Niazian M.R. (2013). "Investigation of nano-clay effect on geotechnical properties of Rasht clay." *Journal of Advanced Science and Technology,* **3**(3), 37-46. http://www.rspublication.com/ijst/june13/5.pdf

Neethu, S.V. and Remya, S. (2013). "Engineering behaviour of nanoclays stabilized soil." In *Proceedings of Indian Geotechnical Conference*, 22-24.

Padidar, M., Jalalian, A., Asgari, K., Abdouss, M., Najafi, P., Honarjoo, N., and Fallahzade, J. (2017). "The impacts of nanoclay on sandy soil stability and atmospheric dust control." *Agriculturae Conspectus Scientificus*, **81**(4), 193-196. https://hrcak.srce.hr/file/264558

Shaikh, A., Ruff, J.F., and Abt, S.R. (1988). "Erosion rate of compacted Na-montmorillonite soils." *Journal of Geotechnical Engineering*, **3**, 296-305. https://worldcat.org/title/5711421467

Spagnoli, G. (2018). "A review of soil improvement with non-conventional grouts." *International Journal of Geotechnical Engineering*, **15**(3), 273-287. https://doi.org/10.1080/19386362.2018.1484603

Tabarsa, A., Latifi, N., Meehan, C.L., and Manahiloh, K.N. (2018). "Laboratory investigation and field evaluation of loess improvement using nanoclay — A sustainable material for construction." *Construction and Building Materials,* **158**, 454-463. https://doi.org/10.1016/j .conbuildmat.2017.09.096

Taghavi, P., Mousavi, S.F., Shahnazari, A., Karami, H., and Shoshpash, I. (2019). "Experimental and numerical modeling of nano-clay effect on seepage rate in earth dams." *International Journal of Geosynthetics and Ground Engineering*, **5**(1), 1-8. https://doi.org/10.1007/s40891-018-0152-8

Wahl, T.L. (2010). "Relating HET and JET test results to internal erosion field tests." *Joint federal interagency conference on sedimentation and hydrologic modeling*, Las Vegas, USA.

Wan, C.F. and Fell, R. (2004). "Investigation of rate of erosion of soils in embankment dams." *Journal of Geotechnical and Geoenvironmental Engineering*, ASCE, **130**(4), 373-380. https://doi.org/10.1061/(ASCE)1090-0241(2004)130:4(373)

Zhang, Q., Chen, S., and Deng, Z. (2017). "Numerical model for homogeneous cohesive dam 470 breaching due to overtopping failure." *Journal of Mountain Science*, **14**(3), 571-580. https://doi.org/10.1007/s11629-016-3907-5

Zomorodian, S.M.A. and Momen, M. (2018), "Experimental study of the effectivness of nano-silica additive on the internal erosion of divergent soils." *Sharif Journal of Civil Engineering,* **34.2**(1.2), 143-148. https://doi.org/10.24200/J30.2018.1356

Zomorodian, S.A., Shabnam, M., Armina, S., and O'Kelly, B.C. (2017), "Strength enhancement of clean and kerosene-contaminated sandy lean clay using nanoclay and nanosilica as additives." *Applied Clay Science*, **140**, 140-147. https://doi.org/10.1016/j.clay.2017.02.004